

Characterization of a Ca-Dependent Maxi K Channel in the Apical Membrane of a Cultured Renal Epithelium (JTC-12.P3)

H.A. Kolb[†], C.D.A. Brown^{‡,*}, and H. Murer[‡]

[†]Faculty of Biology, University of Konstanz, D-7750 Konstanz, Federal Republic of Germany, and [‡]Department of Physiology, University of Zürich-Irchel, CH-8037 Zürich, Switzerland

Summary. A Ca and potential-dependent K channel of large unit conductance was detected in the apical membrane of JTC-12.P3 cells, a continuous epithelial cell line of renal origin. The open probability of the channel is dependent on membrane potential and cytoplasmic-free Ca concentration. At cell-free configuration of the membrane patch, the open probability shows a bell-shaped behavior as function of membrane potential, which decreases at larger depolarization. With increasing Ca concentration, the width of the bell-shaped curve increases and the maximum shifts into the hyperpolarizing direction. For the first time the kinetics of this channel was analyzed under cell-attached conditions. In this case the kinetics could sufficiently be described by a simple open-closed behavior. The channel has an extremely small open probability at resting potential, which increases exponentially with depolarization. The low probability induces an uncertainty about the actual number of channels in the membrane patch. The number of channels is estimated by kinetic analysis. It is discussed that this K channel is essential for the repolarization of the membrane potential during electrogenic sodium-solute cotransport across the apical membrane.

Key Words maxi-K(Ca) channel · open probability · burst kinetics · apical membrane · on-cell patch clamp

Introduction

Identification of the cellular mechanisms by which renal epithelial cells transport K ions has been the subject of numerous investigations over the last few years. Of particular interest has been the identification of large K-conductive pathways in the apical membrane of cortical collecting duct cells (Koepfen, Biagi & Giebisch, 1983; O'Neil & Sansom, 1984) and in the basolateral membrane of renal proximal tubular cells (Bello-Reuss, 1982; Biagi, Kubota, Sohtell & Giebisch, 1981). With the advent of the patch-clamp technique (Hamill et al., 1981) and the subsequent investigation of the physical properties of single ionic channels in a wide range of

tissues, several classes of K channels have been identified (Latorre & Miller, 1983; Petersen & Maruyama, 1984). For renal epithelium, Ca-dependent K channels (K(Ca) channel) have recently been reported to be present in the apical membrane of cortical collecting duct cells (Hunter, Lopes, Boulpaep & Giebisch, 1984) and in both the apical and basolateral membrane of renal proximal tubular cells (Gögelein & Greger, 1984). But in these cell membranes, a K(Ca) channel of a single-channel conductance of about 90 pS is found whereas, as described below, we could identify a K(Ca) channel of about 220 pS.

In this report we have investigated the properties of the apical membrane of an established renal epithelial cell line, JTC-12, using the patch-clamp technique (Kolb, Brown & Murer, 1985). The JTC-12 cell line was established from the kidney of a cyanomolgous monkey (Ishizuka et al., 1978) and, like a number of other epithelial cell lines (Handler, Perkins & Johnson, 1980), it has remained differentiated in culture exhibiting a hormonal sensitivity (Ishizuka et al., 1978), transepithelial electrical resistance and transport properties (*unpublished observations*) normally associated with the proximal tubule.

The major result of this work is the identification of the Ca-dependent K channel of large unit conductance, which is well known as the Ca-dependent maxi-K channel in membranes of excitable cells (*cf.* Latorre & Miller, 1983). The single-channel properties of this channel were extensively studied on inside-out oriented myotube membranes of rat (Magleby & Pallotta, 1983a,b) and also on myotubes of embryonic chicken (Kolb, 1986). In this paper, using the cell-free configuration of the membrane patch, the percentage of channel open time was measured as function of membrane potential and Ca^{2+} . It was found that the Ca- and potential-dependent gating properties of the channel

* Present address: Department of medicine, Hope Hospital, Eccles Old Road, Salford, M6 8HD, U.K.

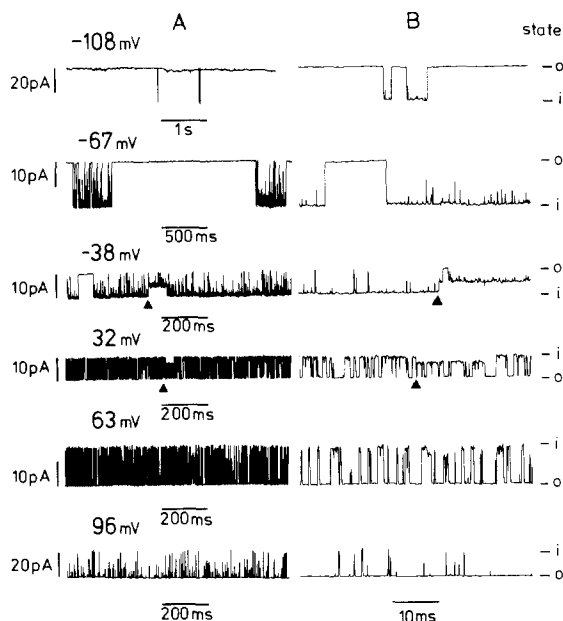


Fig. 1. Current records at different membrane potentials as indicated. Inside-out membrane configuration with symmetrical high-K solution on both sides of the membrane. The bath additionally contained 10^{-7} M Ca^{2+} (0.55 mM CaCl_2 , 1.1 mM EGTA). In columns A and B different time scales are used. For better comparison in B the time scale was left constant, whereas in A the time scale was adjusted to the frequency of channel openings. At -38 and 32 mV current amplitudes of lower level are marked, respectively. On the right-hand side the channel states were marked: (o) for closed state and (i) for the fully open state. At 96 mV single-channel events are only partially resolved due to the filtering

are similar to the results obtained on membranes of excitable cells (Barrett, Magleby & Pallotta, 1982) and to K channels from rat muscle incorporated into planar lipid bilayers (Moczydlowski & Latorre, 1983). But in addition, we observed a decrease of the percent of channel open time at larger depolarizing potentials. This result could be described by the use of a three-state reaction scheme, but not by the potential-dependent gating kinetics outlined by Moczydlowski and Latorre for this type of channel.

For the first time a kinetic analysis is presented in the cell-attached configuration of the patch pipette at physiological cytoplasmic composition. We carefully considered the problem that the actual number of channels in the membrane patch contributing to the recorded current pattern is not known. The possible role of this channel in the overall ionic transport across the apical membrane is discussed.

Materials and Methods

CELL MATERIAL

JTC-12.P3 cells (Takaoka et al., 1962) were obtained from Dr. T. Matsumura, Tokyo (Japan) at serial passage 81 and were main-

tained in culture between passage 85 and 100. The growth medium was DM 160 (Katsuta & Takaoka, 1970) containing 2 mM glutamine, 50 IU/ml penicillin, 50 $\mu\text{g}/\text{ml}$ streptomycin, 10% (vol/vol) fetal calf serum. The cells (seeding density $0.5 - 1.0 \times 10^5/\text{ml}$) were grown in 35 mm diameter petri dishes for 5 to 6 days to confluent monolayers. For the experiments, the cells were grown on glass coverslips in petri dishes. At start of the experiments, the cover slips were broken into pieces and placed into a miniature chamber (see below).

PATCH-CLAMP EXPERIMENTS

Patch-clamp experiments were carried out according to the method of Neher and Sakmann (cf. Hamill et al., 1981). The experiments were performed under cell-attached configuration of the micropipette and also on inside-out membrane patches. In the latter case, the free Ca concentration on the cytoplasmic side of the membrane $[\text{Ca}^{2+}]_i$ could be varied, and the influence on the channel open probability determined. To achieve a consistent convention for the notation of potentials throughout all the experiments, the potentials were denoted as membrane potentials and were referred to a potential of 0 mV of the micropipette. In the cell-attached configuration of the pipette, the resting membrane potential contributes to the actual membrane potential. For clearer presentation, a resting membrane potential of -50 mV [in analogy to proximal tubular cell (Frömter, 1979)] was considered in these experiments. Positive currents from the cytoplasm to the pipette are drawn as upward currents. The current records were stored on an FM tape recorder (Racal Store 4) with a frequency response of DC to 20 kHz. The records were actively low-pass filtered (Krohn-Hite Model 3342) at a cut-off frequency (-3 db frequency) of usually 3 kHz.

ELECTROLYTE SOLUTIONS

For current records in the cell-attached configuration, the bath contained Krebs-Ringer solution of (mM): 137 NaCl, 5.4 KCl, 0.5 NaH_2PO_4 , 1.2 MgCl_2 , 2.8 CaCl_2 , 10 glucose, 14 Tris buffered to pH 7.3 with HCl.

At the start of the experiments, using the inside-out configuration, the bath contained Krebs-Ringer solution, which was varied by continuous perfusion of the $100 \mu\text{l}$ miniature chamber with a high-K medium (mM): 145 KCl, 1.13 MgCl_2 , 20 HEPES-KOH, pH 7.3). To obtain levels of bath $[\text{Ca}^{2+}]$ below 10^{-5} M, 1.1 mM EGTA and the following concentrations of CaCl_2 were added to this medium: 1.08 mM for 4×10^{-6} M Ca^{2+} , 0.55 mM for 1×10^{-7} M Ca^{2+} . The effective free Ca concentration was calculated using an apparent dissociation constant of 10^{-7} M for Ca-EGTA and $10^{-1.8}$ M for Mg-EGTA (Portzehl, Caldwell & Rüegg, 1964). For a $[\text{Ca}^{2+}]$ well below 10^{-7} M we added to a MgCl_2 , CaCl_2 -free solution of (mM): 145 KCl, 10 glucose, 20 HEPES-KOH and 1.0 EDTA at pH 7.3. The ionic selectivity was investigated on inside-out membrane preparations, where potassium in the high-K medium was replaced by equal amounts of NaCl.

The patch-electrode contained the high-K medium with no CaCl_2 added in all experiments. Experiments were performed at room temperature of $20-23^\circ\text{C}$.

DATA ANALYSIS

For the estimation of the percentage of time during which a channel is open, amplitude histograms of current fluctuations were determined (Hewlett Packard 5420A Digital Signal Analyzer) at a sample time of $9.8 \mu\text{sec}$. The area of the Gaussian-like

distributed amplitudes of the leak current and the unitary channel currents was calculated on line (Hewlett Packard 9825A). The ratio of the corresponding areas was taken as estimate of the time during which one channel is open (P). The actual number of K channels, which was estimated by fitting the sequence of amplitude maxima by a geometric series, was taken into account for the calculation of P .

For kinetic analysis, the current fluctuations were recorded on a tape recorder (*see above*) and played back at 1/32 speed into a strip-chart recorder (Gould Brush 2200S). The open-closed events were digitized using a Hewlett Packard 9874A digitizer, applying the half-amplitude threshold analysis (Colquhoun & Sigworth, 1983). Sojourns within single-channel current pulses to lower current levels lasting less than 300 μsec were regarded as open times. Sojourns to larger current levels were treated in analogy. The derived frequency distributions were fitted by exponential functions using a least squares routine.

Results

PATCH-CLAMP RECORDS FROM INSIDE-OUT CONFIGURATION

Figure 1 shows a current record of an active membrane patch in the inside-out configuration at different membrane voltages. The free Ca^{2+} concentration on the cytoplasmic side of the membrane ($[\text{Ca}^{2+}]$) was adjusted to 10^{-7} M. It may be seen from Fig. 1 that one channel is active and that the kinetics is a function of applied voltage. By estimation of the percentage of time during which this channel is open ($P(U)$) one obtains an about symmetrical dependence on the voltage amplitude (U), independent on the selected polarity (*see also* Fig. 1). The corresponding functional relationship of $P(U)$ is represented by curve C in Fig. 2. The function shows a symmetrical course around a voltage of -25 mV. But as Fig. 1 indicates, the corresponding kinetic pattern is not symmetrically distributed. The symmetrical behavior of $P(U)$ could be determined for the Ca^{2+} -concentration range of 1 mM to $0.1 \mu\text{M}$ (Fig. 2, curves A–C.). At $[\text{Ca}^{2+}]$ below 10^{-7} M, only the onset of the probably bell-shaped function $P(U)$ (curve D in Fig. 2) could be measured, at hyperpolarizing voltages it could not be recorded due to the low activity. Figure 2 shows furthermore that the width of the function $P(U)$ increases with increasing free cytoplasmic calcium. An increase of $[\text{Ca}^{2+}]$ also causes an increase of $P(U)$ at constant voltage.

At symmetrical high-K electrolyte (Materials and Methods) on both sides of the membrane, a linear current-voltage relationship (i function) is found for the channel unit amplitude in a voltage range of about -100 to 100 mV with an expected zero current potential of 0 mV. For the corresponding single-channel conductance $\gamma = 220 \pm 17$ pS ($n = 24$) is obtained, independent of the free Ca concentration. In some experiments a subconductance

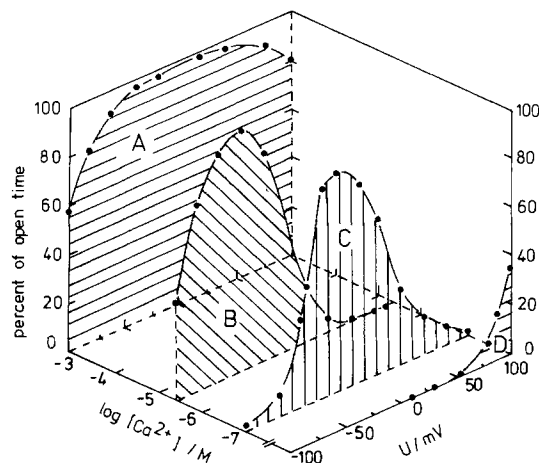


Fig. 2. Three-dimensional plot of percent of time during which a channel is open versus membrane potential and cytoplasmic-free calcium (Materials and Methods). The inside-out configuration of the membrane was used with symmetrical KCl (145 mM) on both sides. The curves were drawn by hand. For clearer presentation the curve at 5×10^{-5} M Ca^{2+} (*see* Table 2) was omitted, which fits well into the sequence of curves A–C. For curve D the bath contained (mM): 145 KCl, 1 EDTA, 10 glucose, 20 HEPES-KOH at pH 7.3. Each curve represents an average of 2 to 4 experiments

level could be observed (*see* marked current steps in Fig. 1). The corresponding i - V curve was linear and showed a reversal potential of also 0 mV. For the conductance ratio of subconductance state to fully open state, a value of 0.58 ± 0.02 ($n = 5$) was derived.

For measurements of ionic selectivity, $[\text{Ca}^{2+}]$ was adjusted to 10^{-7} M in a high-K medium. A change of KCl in the bath from 145 to 25 mM by equal amounts of NaCl shifted the zero current potential by 32 ± 3 mV ($n = 3$). The sign and amplitude of the potential shift indicates a potassium selective behavior of the described channel.

PATCH-CLAMP RECORDS IN THE CELL-ATTACHED CONFIGURATION

Cell-free records of the Ca-dependent K channel offer no information on the actual free cytoplasmic Ca concentration which activates the channel at rest, and about the corresponding kinetic pattern. Therefore, we measured the channel-induced current fluctuations also in the cell-attached configuration of the pipette. The channel could only be detected at larger depolarizing membrane potentials, which cause longer channel lifetimes and larger opening probabilities (*see* Discussion). Figure 3 shows the current pattern of a typical experiment at different membrane potentials. For calculation of the membrane potential, a constant resting potential of -50 mV was taken into account (Materials and

Methods). Figure 3 shows that besides the channel of large current amplitude a second population of channels with a small amplitude and an obviously distinguishable current pattern appears. Both types of channels could be observed simultaneously and also independently from each other (*see* time-expanded current trace at 66 mV in Fig. 3). The corresponding current-voltage relations are given in Fig. 4. For the channel of smaller amplitude a conductance of $\gamma = 24 \pm 2$ pS ($n = 4$) is derived, whereas for the channel of larger amplitude $\gamma = 215 \pm 27$ pS ($n = 6$) is obtained. If the measured i - U curves of Fig. 4 are linearly extrapolated to the zero current value, a corresponding potential of -27 mV is found for both channel types. To support the hypothesis that the channel of large amplitude is a Ca-dependent K channel, the current pattern was measured after changing from the cell-attached configuration (Fig. 3) to the inside-out configuration (Fig. 5), without changing the Krebs-Ringer solution of the bath. By the now applied potassium gradient (5.4 mM KCl in the bath and 145 mM KCl in the pipette), only the inward-directed cationic current could be recorded. As expected, the high Ca concentration of the bath (1.2 mM) causes the channel to adopt the open state more often. From the data of Fig. 5, a zero current potential of 75 mV could be extrapolated. Assuming a pure K selectivity of the channel, the Nernst equation would yield 82 mV. In Fig. 5, the channel of smaller current

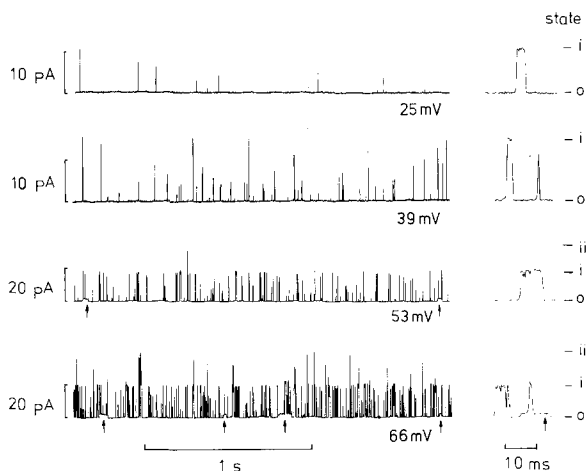


Fig. 3. On-cell current records at different applied membrane potentials. Membrane potentials were calculated as described in Materials and Methods. The simultaneous appearance of a second channel population is marked in some cases by an arrow. At each potential channel events are also shown on an expanded time scale on the right-hand side. States of the K(Ca) channel are named as: (o) closed state, (i) fully open state, (ii) two superimposed fully open states. The channel of smaller amplitude was omitted for this notation

amplitude (*see* arrows in Fig. 5) is also visible. Its kinetics appears to be dependent on $[Ca^{2+}]_i$, too, but will be considered in detail elsewhere. Also for this channel type, a zero current potential of about 75 mV is obtained. Therefore, the channel seems to be selective for potassium as well.

In the cell-attached pipette configuration, a more detailed kinetic analysis for the Ca-dependent K channel was performed. The analysis allows an estimate of the kinetic single channel properties at resting membrane potential.

As Fig. 3 indicates, the single-channel current pulses are interrupted by gaps of very different durations. At smaller depolarization (≤ 50 mV, Fig. 3), the current fluctuations show a pattern of well-distinguishable channel openings and closed times between single-channel pulses. At higher depolarization (> 50 mV), the current pattern of the open state indicates that short-lived transitions to lower current states occur, which are only partially resolved due to the limited time resolution of the set up (Ma-

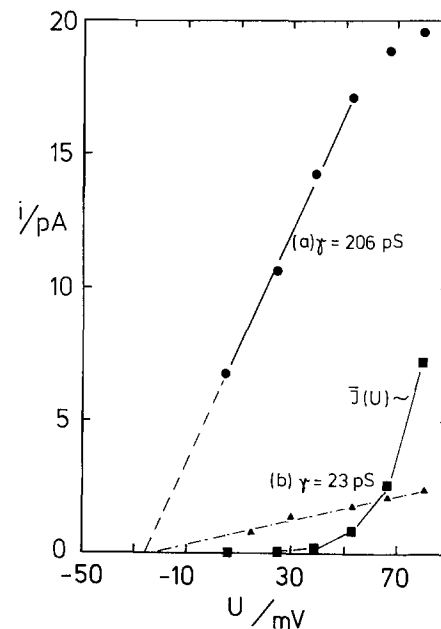


Fig. 4. Current amplitudes (i) versus applied membrane potential of single-channel events. The current values were obtained from the evaluation of corresponding amplitude histograms. The drawn line represents a fit of the ohmic relation to the linear part of the i - U curve for the large current amplitudes (●) which yields (a): $\gamma = 206$ pS. For the second type of current amplitudes (▲) (*see* arrows in Fig. 3) it was derived (b): $\gamma = 23$ pS. By linear extrapolation of curves (a) and (b) a common zero potential of -27 mV is found. The data were as used for Fig. 3. The points (■) give the mean contribution of one K(Ca) channel to the macroscopic current. The mean current was calculated by the relation $\bar{J} = i(U) \cdot p(U)$ where $i(U)$ denotes the single-channel current (points (●)) and $p(U)$ the corresponding channel open probability (Table 2)

terials and Methods). The corresponding frequency histograms could be described by a single exponential distribution for all potentials applied and analyzed times above 300 μsec . Figure 6a shows frequency histograms of open and closed times which were analyzed at 66 mV. Each frequency distribution yields a characterization time constant of either the closed state (τ_0) or the open state (τ_1). The corresponding time constants are given in Fig. 6b and Table 2. As the figure indicates a single exponential dependence on membrane potential is obtained which fits the relation given by the Eyring rate theory:

$$\tau_i(U) = \tau_i(0) * \exp(\delta_i * U) \quad (i = 0, 1) \quad (1)$$

where $\tau_i(0)$ denotes the mean time constant at zero membrane potential and δ_i the potential sensitivity in mV^{-1} of either the closed or open state. The fitted values are given in the legend of Fig. 6b.

Discussion

This paper examines the Ca- and voltage-dependent activation of a K channel of large unit conductance (K(Ca) channel), observed in the apical membrane of renal epithelial cells (JTC-12.P3). In the first part the analyzed single-channel properties are discussed, focussing on the measurement of the channel open probability in the cell-free and cell-attached pipette configuration. The possible role of

this channel in overall ionic transport across the apical membrane is discussed at the end of this section.

At inside-out configuration and symmetrical high KCl solution on both sides of the membrane a single-channel conductance of about 200 pS was obtained. In some cases, the current pattern showed the occurrence of a sublevel with a conductance of

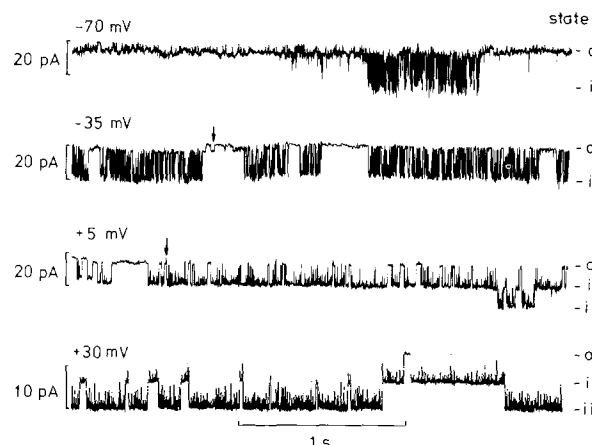


Fig. 5. Current records at different membrane potentials. The data were obtained from the same membrane patch as used for Fig. 3 after changing to the inside-out configuration. Bath and pipette solution were as given for Fig. 3. A second type of channel of lower current amplitude appears; some events are marked by arrows. States of the K(Ca) channel: (o) closed state, (i) fully open state, (ii) two superimposed, fully open states

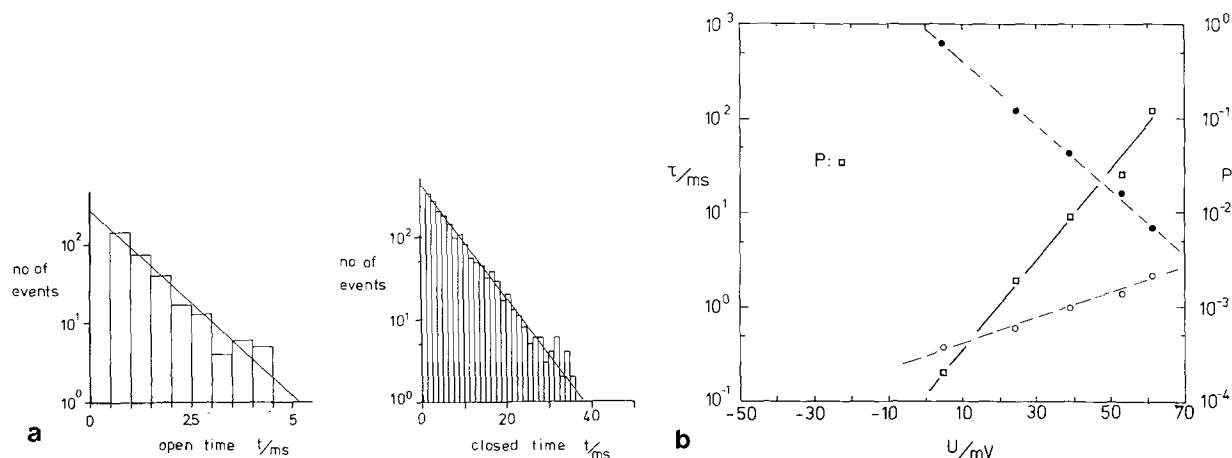


Fig. 6. (a) Frequency histogram of lifetimes of current fluctuations in state (o) (closed state) and in state (i) (fully open state) at a membrane potential of 66 mV (see for notation Fig. 3). All transitions shorter than 300 μsec were discarded. (Materials and Methods). The straight line represents a single exponential fit, yielding a characteristic mean open time of 2.1 msec and a mean closed time of 6.3 msec. The experimental conditions were as used for Fig. 3. (b) Mean lifetime of current fluctuations in state o (τ_o , \bullet), closed state) and in the open state i (τ_i , \circ) one channel fully open) as function of membrane potential. Regression lines were fitted to the semilogarithmic plot of these values. Using Eq. (1), the following parameters are derived: $\tau_1(0) = 3 \times 10^{-4}$ sec, $\delta_1 = 0.032 \text{ mV}^{-1}$; $\tau_o(0) = 96 \text{ msec}$; $\delta_o = -0.079 \text{ mV}^{-1}$. The experimental conditions were as used for Fig. 3. Also, the channel open probability p of an individual channel is plotted (\square). The corresponding scale is given on the right ordinate. Values are taken from Table 2

Table 1.

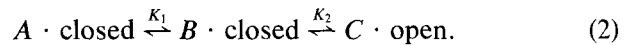
$[Ca^{2+}]_i/M$	10^{-7}	4×10^{-6}	5×10^{-5}	10^{-3}
V_s/mV	18.9	44	46	36
$K_1(0)$	9.3×10^{-4}	6×10^{-4}	8×10^{-4}	2×10^{-3}
δ_1/mV^{-1}	0.11	0.05	0.05	0.05
$K_2(0)$	5.6×10^3	1.7×10^5	7.5×10^2	1.5
δ_2/mV^{-1}	0.18	0.15	0.1	0.1

Description of probability that one channel is open as function of membrane potential (U) by Eq. (3). The potential dependence of the equilibrium constants $K_1(U)$ and $K_2(U)$ was described in analogy to Eq. (1) by $K_i(U) = K_i(0) \cdot \exp(\delta_i \cdot (U - U_s))$ ($i = 1, 2$). At different free calcium concentrations the values for K_i , δ_i and U_s were obtained by least squares fitting of Eq. (3) to the data of Fig. 2. The table also contains the values derived at $5 \times 10^{-5} M Ca^{2+}$, which are not shown in Fig. 2.

about 125 pS (Fig. 1). A similar subconductance level was observed for this channel in rat myotubes (Barrett et al., 1982) and for an anionic channel of large unit conductance (340–450 pS) in embryonic chicken myotubes (Schwarze & Kolb, 1984).

By varying of Ca^{2+} on the cytoplasmic side of the channel and the membrane potential (U), a corresponding influence on the percent of time during which a channel is open ($P(U)$) could be measured (Fig. 2). The results can be compared with those reported for the K(Ca) channel in rat myotubes (Barrett et al., 1982) and for the isolated K(Ca) channel from rat muscle incorporated into lipid bilayer membranes (Moczydlowski & Latorre, 1983). At less membrane depolarization and low $[Ca^{2+}]_i$ ($<10^{-7}$), significantly larger values of $P(U)$ are found in JTC-12 membranes compared with the results obtained on excitable cell membranes. This finding can qualitatively be explained by higher affinity binding of Ca to the channel protein in this epithelial membrane. At larger depolarization, $P(U)$ declines yielding an about symmetrical and bell-shaped course, whereas in excitable membranes $P(U)$ asymptotically reaches the value one for the permanently channel open state. A similar bell-shaped behavior of $P(U)$ has already been observed for an anionic channel in macrophages and embryonic chicken myotubes (Schwarze & Kolb, 1984). For a theoretical description, the observed current pattern has to be suitably described in terms of chemical reaction kinetics. Moczydlowski and Latorre proposed (1983) a linear kinetic scheme of four states with two closed and two open channel states for the description of the voltage-dependent gating reactions. For optimal opening, the channel must have two bound Ca ions, whereby the Ca binding steps were assumed to be the only voltage-dependent reaction steps. But their data do not explain the observed bell-shaped behav-

ior of $P(U)$. The minimum kinetic diagram we found for a description of the bell-shaped course of $P(U)$ consists of at least three channel states with two voltage-dependent reaction steps



From this hypothetical reaction scheme, $P(U)$ ($= 100 \cdot p(U)$) is derived

$$p(U) = \frac{1}{1 + K_2(U) \cdot [1 + K_1(U)]}. \quad (3)$$

K_1 , K_2 denote the dissociation constant of the corresponding reaction step and $p(U)$ is the probability to find a channel in the open state. It was found that Eq. (3) suitably describes the behavior of $P(U)$ for all $[Ca^{2+}]_i$ used. The values of K_1 and K_2 , which were derived by fitting of Eq. (3) to the data of Fig. 2, are given in Table 1. We propose from our data that at high depolarization further voltage-dependent reaction steps besides the Ca binding reactions must be taken into account for an explanation of the decrease of $P(U)$.

At cell-attached configuration of the pipette and physiological incubation conditions, one is faced with the problem that the probability for a channel to adopt the open state is rather low (see below). Therefore, at first we analyzed the channel kinetics, which allows an estimation of the channel open probability. Magleby and Pallotta (1983a) proposed from the kinetic analysis of the K(Ca) channel at inside-out membrane patches a state diagram of at least three closed states and two open states, which correspond to three mean closed times and two mean open times. But as shown in Fig. 6a, the frequency distributions of channel open times and closed times showed a single-exponential behavior for events lasting longer than 500 μsec for on cell records. It is interesting to note that in the limit of low $[Ca^{2+}]_i$ ($<10^{-7} M$), which would correspond to a physiological Ca concentration, the data of Magleby and Pallotta indicate a vanishing difference between long and short mean open times, which would fit our data. But the reported difference between the long and short mean shut interval increases at low $[Ca^{2+}]_i$. Therefore, for on-cell records of the K(Ca) channel one should expect in addition to the observed long lasting closed interval also an intermediate one around 1 msec and a short one in the range of 300 μsec . In our records the latter ones were not observed, but we cannot exclude from our data that mean time constants below 300 μsec exist. For a detailed comparison of the kinetics it has to be considered that so far a kinetic

Table 2.

U/mV	4	24	34	53	66	-50
Experimental values						
τ_0 /msec	625.2	110	42.3	16.1	6.4	
τ_1 /msec	0.37	0.6	0.98	1.18	2.1	
τ_2 /msec	—	—	—	0.7	0.9	
p_2	—	—	—	1.7×10^{-3}	1.9×10^{-2}	
Theoretical values						
α /sec ⁻¹	2.7×10^3	1.7×10^3	1×10^3	8.1×10^2	37.0	1.2×10^4
β /sec ⁻¹	0.53	3.0	7.9	21.1	52.0	0.008
$\tau_2(3)$ /msec	0.19	0.3	0.49	0.6	1.3	0.03
p	2×10^{-4}	1.8×10^{-3}	7.8×10^{-3}	2.5×10^{-2}	0.12	5×10^{-7}
$p_2(3)$	1.2×10^{-7}	9.9×10^{-6}	1.8×10^{-4}	1.8×10^{-3}	4.0×10^{-2}	
$p_3(3)$	7.7×10^{-12}	6.0×10^{-9}	4.7×10^{-7}	1.6×10^{-5}	1.9×10^{-3}	

Mean channel closed time (τ_0) and open time (τ_1) of Fig. 6b as well as the mean lifetime for two simultaneously open channels (τ_2) (see state *ii* in Fig. 3) of on-cell records performed at different membrane potentials. The probability p_2 was estimated from the total time that two channels are simultaneously open divided by the observation time and corrected for the events lasting less than 300 μ sec. The rate constants α , β of Eq. (4) were calculated by Eq. (5), assuming that three K(Ca) channels are active in the membrane patch. $\tau_2(3)$ is derived from Eq. (5) for $n = 3$ and $j = 2$. The steady-state probability $p_j(n)$ ($j = 2, 3; n = 3$) was obtained from the binomial distribution. For the channel open probability of an individual channel the relation $p = \beta/(\alpha + \beta)$ was used. In the last column parameter values are noted at resting membrane potential, which were derived by extrapolation of the corresponding potential dependence. For further explanations see text.

analysis of this channel has only been performed on inside-out membrane patches, omitting sodium ions on the cytoplasmic side. From the data of Yellen (1983) one can suppose that cytoplasmic Na^+ in the millimolar range significantly modulates the channel kinetics in on-cell records. It turned out that in all on-cell records at least two simultaneously fluctuating channels of equal amplitude became detectable at larger depolarization (Fig. 3). For calculation of $P(U)$ of an individual channel, the actual number of channels in the membrane patch has to be known. An analytical solution of this many-channel problem, including the bias of the limited time resolution of the experimental set up, is not known. Our treatment of the many-channel problem is based on the observation that, as a first approximation, a two-state scheme can be used for the description of the channel fluctuations in on-cell records (see also Fig. 6a)



The observed closed times (τ_0) and open times (τ_1) (Fig. 6) can then be given as function of number of channels (n) generating the current pattern and of α and β (Kolb, 1986)

$$\tau_j = (j \cdot \alpha + (n - j) \cdot \beta)^{-1} \quad (j = 0, 1, \dots, n). \quad (5)$$

For derivation of Eq. (5), the assumption was used that the K(Ca) channels are indistinguishable and noninteracting. Knowledge of α and β allows an estimate of the channel open probability ($p = \beta/(\alpha + \beta)$). To estimate the actual number of channels in the patch, also the probability, $p_j(n)$ that out of n channels $j \leq n$ are simultaneously open, was measured and compared with the expectation from the binomial distribution (Colquhoun & Hawkes, 1983). At larger depolarization, p_2 could be measured (Table 2). For $n = 3$ we obtained the best fit to the experimental values given in Table 2. Using Eqs. (5) and (1), α and β could be derived as function of membrane potential. The following set of parameters was obtained by linear regression: $\beta(0) = 3.8 \times 10^{-3} \text{ msec}^{-1}$, $\delta_0 = 0.077 \text{ mV}^{-1}$, $\alpha(0) = 3.1 \text{ msec}^{-1}$, $\delta_1 = -0.027 \text{ mV}^{-1}$. The corresponding mean values of five different experiments are: $\beta(0) = (1.3 \pm 0.6) \times 10^{-3} \text{ msec}^{-1}$, $\delta_0 = 0.07 \pm 0.008 \text{ mV}^{-1}$, $\alpha(0) = 4.4 \pm 1.0 \text{ msec}^{-1}$, $\delta_1 = -0.023 \pm 0.003 \text{ mV}^{-1}$. Through extrapolation of $p(U)$ in Fig. 6b, a value of 5×10^{-7} was found for the channel open probability at resting membrane potential which corresponds to a mean channel open time of about 70 μ sec and a mean closed time of 130 sec (see Table 2). Therefore, an estimate of the actual channel number in on-cell records can only be derived at large depolarization, where the channel open probability reaches the 1% level. The extrapolated value of $p(U)$ is at least two orders of magnitude lower as found in

inside-out measurements at 10^{-7} M Ca^{2+} on excitable cell membranes. The discrepancy could be caused by neglecting the cytoplasmic sodium in cell-free records, since sodium ions block the K(Ca) channel on the same time scale (Yellen, 1984) of the lifetime of the open (Ca occupied) channel state, which reduces the steady-state open probability.

Despite the large single-channel conductance, the low open probability reduces the mean macroscopic current contribution \bar{J} of a K(Ca) channel at rest to less than 20 fA. By depolarization of 100 mV, \bar{J} increases to about 1 pA, and further depolarization causes a steep increase of \bar{J} (Fig. 4). At larger depolarization \bar{J} should decrease again, as expected from the bell-shaped behavior of $P(U)$ (Fig. 2). But in on-cell experiments, those large depolarizing membrane potentials could not be achieved.

In the following we would like to consider some of the possible physiological roles such a channel could play in the JTC-12.P3 cell epithelium and by analogy in the renal proximal tubule. One such role for a voltage and Ca-gated K conductance is the maintenance of the apical membrane potential, and hence the driving force, during Na/solute cotransport across the apical membrane of these epithelia.

It is well known that the renal proximal tubule is the site of a number of Na-dependent solute cotransport systems for both organic and inorganic solutes (Frömter, 1979; Ullrich, 1979) and the majority of cotransport systems are rheogenic (usually carrying a net positive charge across the apical membrane) (Murer & Kinne, 1980; Burckhardt & Murer, 1980). Therefore, during periods of high transport activity, the net result of solute reabsorption is a depolarization of both the apical and the basolateral membrane potential (Biagi et al., 1981) and a concomitant decrease in the driving force for solute uptake across the apical membrane (a decreased electrochemical gradient for Na). Since the K channel described in this paper is predominantly gated by voltage (as are the majority of Ca-activated K channels described so far (cf. Petersen & Maruyama, 1984)), it is possible to envisage a scheme in which a voltage-sensitive K channel is used to buffer fluctuations of membrane potential due to different solute loads and to maintain an optimum electrochemical gradient for Na-dependent rheogenic solute cotransport. In this scheme, the probability of the channel being in an open state increases as the apical membrane depolarizes, resulting in a net efflux of K from the cell and a hyperpolarization of the membrane potential. As the membrane potential returns to a more normal value the probability of channel opening is reduced. In this way both absorption of solute and loss of cellular K are kept under control. Secondly, the Ca_i^{2+}

sensitivity of the channel could be utilized in a similar manner, since a decreased electrochemical gradient for Na could effect the efficiency of Ca extrusion from the cell via the Na:Ca exchanger, resulting in a slight rise in intracellular free Ca^{2+} , which could activate the K channel in a similar manner to a decrease in apical membrane potential.

The authors would like to thank Mrs. M. Solleder for her excellent technical assistance and Mrs. K. Malmström for the preparation of the JTC-12.P3 cells. C.D.A. Brown was supported by the Royal Society (London). The work was supported by the Sonderforschungsbereich 156 of the Deutsche Forschungsgemeinschaft and by the Schweizerischer Nationalfonds (Grant No. 3.266.082).

References

- Barrett, J.N., Magleby, K.L., Pallotta, B.S. 1982. Properties of single calcium-activated potassium channels in cultured rat muscle. *J. Physiol. (London)* **331**:211–230
- Bello-Reuss, E. 1982. Electrochemical properties of the basolateral membrane of the straight portion of the rabbit proximal renal tubule. *J. Physiol. (London)* **326**:49–63
- Biagi, B.A., Kubota, T., Sohtell, M., Giebisch, G.H. 1981. Intracellular potentials in rabbit proximal tubules perfused in vitro. *Am. J. Physiol.* **240**:F200–F210
- Burckhardt, G., Murer, H. 1980. A cyanine dye as indicator of membrane potential differences in brush border membrane vesicles. Studies with K^+ gradients and Na^+ /amino acid transport. *Adv. Physiol. Sci.* **11**:409–418
- Colquhoun, D., Hawkes, A.G. 1983. The principles of the stochastic interpretation of ion-channel mechanisms. In: *Single Channel Recording*. B. Sakmann and E. Neher, editors. pp. 135–174. Plenum, New York
- Colquhoun, D., Sigworth, F.J. 1983. Fitting and statistical analysis of single channels records. In: *Single Channel Recording*. B. Sakmann and E. Neher, editors. pp. 191–263. Plenum, New York
- Frömter, E. 1979. Solute transport across epithelia: What can we learn from micropuncture studies on kidney tubules? *J. Physiol. (London)* **288**:1–31
- Gögelein, H., Greger, R. 1984. Single channel recordings from basolateral and apical membranes of renal proximal tubules. *Pfluegers Arch.* **401**:424–426
- Hamill, O.P., Marty, A., Neher, E., Sakman, B., Sigworth, F.J. 1981. Improved patch clamp techniques for high-resolution current recording from cells and cell-free membrane patches. *Pfluegers Arch.* **391**:85–100
- Handler, J.S., Perkins, F.M., Johnson, J.P. 1980. Studies of renal cell function using cell culture techniques. *Am. J. Physiol.* **238**:F1–F9
- Hunter, M., Lopes, A.G., Boulpaep, E.L., Giebisch, G.H. 1984. Single channel recordings of calcium activated potassium channels in the apical membrane of rabbit cortical collecting duct. *Proc. Natl. Acad. Sci. USA* **81**:4237–4239
- Ishizuka, I., Tadano, K., Nagata, N., Niimura, Y., Nagai, Y. 1978. Hormone specific responses and biosynthesis of sulfolipids in cell lines derived from mammalian kidney. *Biochim. Biophys. Acta* **541**:467–482

- Katsuta, H., Takaoka, T. 1970. Improved synthetic media suitable for tissue culture of variant mammalian cells. *Methods Cell Biol.* **14**:145–158
- Koeppen, B.M., Biagi, B.A., Giebisch, G.H. 1983. Intracellular microelectrode characterization of the rabbit cortical collecting duct. *Am. J. Physiol.* **244**:F35–F47
- Kolb, H.A. 1986. Ca-activated maxi-K-channel in chicken myotubes: Slow burst kinetics of multi-channel systems, rectification and serial correlation. *Eur. Biophys. J.* (submitted)
- Kolb, H.A., Brown, C.D.A., Murer, H. 1985. A voltage-sensitive K⁺ channel in the apical membrane of a cultured renal epithelium (JTC-12). *Experientia* **41**:830
- Latorre, R., Miller, C. 1983. Conduction and selectivity in potassium channels. *J. Membrane Biol.* **71**:11–30
- Magleby, K.L., Pallotta, B.S. 1983a. Calcium dependence of open and shut interval distributions from calcium-activated potassium channels in cultured rat muscle. *J. Physiol. (London)* **344**:585–604
- Magleby, K.L., Pallotta, B.S. 1983b. Burst kinetics of single calcium-activated potassium channels in cultured rat muscle. *J. Physiol. (London)* **344**:605–623
- Moczydlowski, E., Latorre, R. 1983. Gating kinetics of Ca²⁺ activated K⁺ channels from rat muscle incorporated into planar lipid bilayers. *J. Gen. Physiol.* **82**:511–542
- Murer, H., Kinne, R. 1980. The use of isolated membrane vesicles to study epithelial transport processes. *J. Membrane Biol.* **55**:81–95
- O'Neil, R.G., Sansom, S.C. 1984. Characterization of apical cell membrane Na⁺ and K⁺ conductance of cortical collecting duct using microelectrode techniques. *Am. J. Physiol.* **247**:F14–F24
- Petersen, O.H., Maruyama, Y. 1984. Calcium activated potassium channels and their role in secretion. *Nature (London)* **307**:693–696
- Portzehl, H., Caldwell, P.C., Rüegg, J.C. 1984. The dependence of contraction and relaxation of muscle fibres from the crab *Maia squinado* on the internal concentration of free calcium ions. *Biochim. Biophys. Acta* **79**:581–591
- Schwarze, W., Kolb, H.A. 1984. Voltage-dependent kinetics of an anionic channel of large unit conductance in macrophages and myotube membranes. *Pfluegers Arch.* **402**:281–291
- Takaoka, T., Katsuta, H., Endo, N., Sato, K., Okumura, H. 1962. Establishment of a cell strain, JTC-12, from cynomolgus monkey kidney tissue. *Jpn. J. Exp. Med.* **32**:351–368
- Ullrich, K.J. 1979. Sugar, amino acid and Na⁺ cotransport in the proximal tubule. *Annu. Rev. Physiol.* **41**:181–195
- Yellen, G. 1984. Ionic permeation and blockage in Ca²⁺-activated K⁺ channels of bovine chromaffin cells. *J. Gen. Physiol.* **84**:157–186

Received 20 September 1985; revised 4 April 1986